In-Situ Observation of Bubble Formation in Neat Resin during the Curing Process by Means of X-Ray Computed Tomography

Bernhard PLANK [1], Rhena HELMUS [2], Maxi GSCHWANDTNER [2], Roland M. HINTERHÖLZL [2], Johann KASTNER [1]
[1] University of Applied Sciences Upper Austria, Wels, Austria
[2] TU München, Garching, Germany

Contact e-mail: bernhard.plank@fh-wels.at

Abstract. Because of their outstanding specific strength carbon fibre-reinforced polymers (CFRP) are the favourite material for many lightweight applications, especially in the aeronautic and automotive industries. However, defects like pores in CFRP cannot be completely avoided during manufacturing. For example, moisture in prepreg material can lead to void formation during processing: moisture diffusion forming small water bubbles within epoxy resin that grow or shrink in dependence of pressure and temperature conditions.

This work deals with bubble growth in neat out-of-autoclave (OoA) epoxy resin during processing. OoA prepregs can be processed in conventional ovens without high pressure application. The major concern is that the lack of pressure results in voids: entrapped gases/moisture may not be dissolved in the resin. They can conglomerate and form bubbles which finally reduce the laminate's quality. There are multiple models describing bubble growth and collapse due to diffusion and perfect gas law. The aim of this work is to validate the expected bubble growth by means of X-ray computed tomography (XCT). Therefore a simple in-situ setup was built which cures neat epoxy resin within several hours while providing vacuum and the required temperature. Before the curing process water was injected into the neat resin to induce an entrapped water bubble which can be monitored and measured with a laboratory XCT-System. During the investigations a full XCT-scan was performed every five minutes to observe water bubble behaviour during the curing process.

This work shows that laboratory XCT-Systems are feasible to observe slow curing processes. Usually synchrotron radiation facilities are used for in-situ observations. In our work, the achieved resolution was (58.7 µm)³ voxel size. Results are discussed in the context of analytical models and help to improve understanding of bubble formation during a curing process.

1. Introduction & Motivation

In composites used for aerospace applications it is a fundamental requirement to produce parts with low porosity. The negative effect of defects as well of voids on mechanical properties is already well-known [1-3]. Especially for out-of-autoclave (OoA) manufacturing, void formation is a key challenge due to the missing consolidation pressure

compared to autoclave manufacturing. Therefore, the applied vacuum and hydrostatic resin pressure are the only mechanisms during OoA processing for void reduction. [4].

Reasons for void generation are for example entrapped air between plies during lay-up, volatile content that is released during the curing process, moisture dissolved in the epoxy resin and dry areas within the prepreg material due to incomplete impregnation. [2, 5-10].

Several studies are available in the literature on modelling bubble growth in viscous media. In neat resin the bubble growth is mainly determined by material concentrations and the thermodynamic state of the system. The expansion of a bubble in composite materials is mainly influenced by the fibre bundles, so they are more likely to expand in the fibre direction [11], which causes a deviation from the spherical bubble shape. So the final shape of bubbles and voids greatly depends on the exact fibre architecture and manufacturing process, as shown in several X-ray computed tomography (XCT) investigations [12, 13]. For modelling the bubble formation in epoxy, most authors assume that the effective void volume of the specimen does not change with a spherical approximation of the bubble [5, 6, 14, 15]. This offers a huge mathematical simplification. Based on this, a coupled visco-mechanical and diffusion void growth model was implemented by Helmus et al. [16, 17].

The goal of this work was to close the gap in literature and compare existing knowledge in modelling against experimental results. Due to the limited availability of synchrotron sources and to reduce costs, it was decided to do these investigations with a laboratory XCT system. The fact that in-situ investigations are feasible with laboratory XCT systems had already been shown in several studies [18, 19]. Compromises regarding measurement speed and image quality are necessary.

In this work, an in-situ set-up for a laboratory XCT system was built which enables the processing of neat resin in order to observe the growth behaviour of entrapped air-voids and a single water-bubble to simulate moisture dissolved in epoxy. [20]

2. Experimental Setup

2.1 Neat Epoxy Resin

As neat resin a Cytec Engineered Materials' Cycom® 5320-1 epoxy resin system was used. This resin is usually part of out-of-autoclave (OoA) prepregs allowing typical curing temperatures of ~90° C and curing times of ~12 hours [21]. It was provided as a thin film on a backing paper. To obtain a piece of bulk resin, the resin film was rolled up and formed to a cube of about 1 cm^3. The entrapped air was removed by degassing the bulk resin pieces for about 10 minutes at around 60 °C. After that the degassed bulk resin was cooled down again and stored in a sealed desiccant bag placed in a freezer, before starting the in-situ XCT investigations.

2.2 In-Situ XCT Setup

2.2.1 XCT-Systems and Measurement Parameters

XCT in-situ scans were performed by a Nanotom 180NF XCT device by GE phoenix | x-ray (Wunstorf, Germany). The system has a 180 kV nano-focus tube and a 2304^2 pixel Hamamatsu detector (Hamamatsu City, Japan). The target used was made of molybdenum. To gain short measurement times (5 minutes per scan) a 4 × 4 detector pixel binning mode was used. The resolution (voxel size) was 58.7 µm, the voltage at the nano-focus tube was 60 kV, the measurement current was 220 µA, the integration time at the detector was 125 ms, and the number of projections was 2400 at continuous rotation. Altogether 48 serial

scans were made for the in-situ analysis. The total investigation time was approximately 300 min.

XCT data were reconstructed by means of the Nanotom reconstruction software, including further artefact correction – such as beam-hardening correction of the CT data – and inline median filtering (3x3) of projection images. For further noise reduction, a 5x5x5 median filter was applied to the voxel dataset. The XCT data were evaluated by the commercial software VGStudio Max v2.2 (Volume Graphics GmbH, Heidelberg, Germany).

After in-situ investigations, a further XCT scan was performed on a RayScan 250 E device to generate 3D images of the exact experimental setup shown in Fig. 1. An XCT scan was done at $(47.55)^3$ µm voxel size. The voltage at the micro-focus tube was 190 kV, the measurement current was 225 µA, the integration time was 3000 ms and the number of projections was 1440. As pre-filter, 0.75 mm Sn was chosen.

2.2.2 In-Situ Temperature Chamber

In order to provide an insight into bubble formation within neat resin, a small test rig was built. Due to limited space during XCT scans, the whole setup was built on a 3 mm thick glass tool of approximately 50x80 mm² that enables resin processing in the chamber of an XCT scanner. The neat resin was processed on this glass plate covered with a vacuum bag system. To apply vacuum during the curing process, a two-chamber system was built. A wooden frame was used to stabilize the whole process, while the resin viscosity is low at high temperatures. To seal the whole chamber sealant tape was used, as shown in Fig. 1.

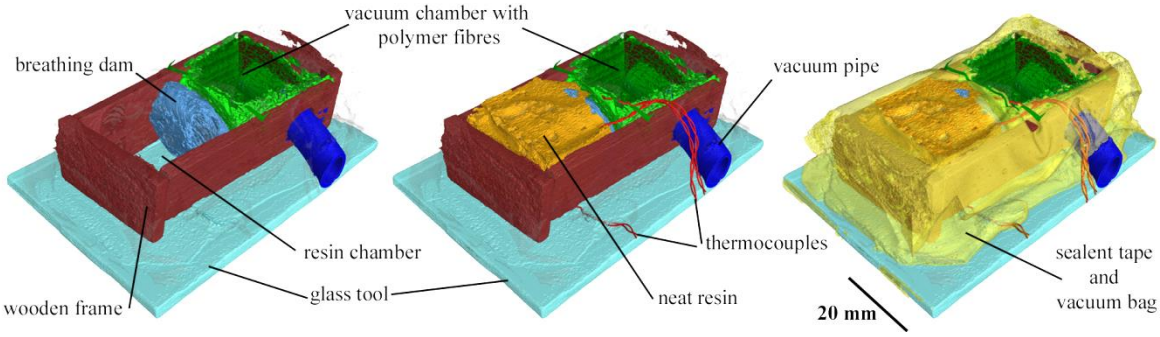

Fig. 1. 3D XCT images of the individual components of the two chamber system on a glass tool for vacuum application. Left: glass tool, breathing dam, resin- and vacuum chamber; Middle: neat resin and position of thermo couples. Right: setup covered with sealent tape and vaccum bag. Images generated after the in-situ experiments with a RayScan 250E XCT-device. Voxel size: $(47.55)^3$ µm

One chamber contains a cube of neat resin while the other is filled with polymer fibres, acting as a distribution helper for the vacuum over the whole setup, and is connected to the vacuum port. In order to connect the resin chamber to the vacuum port while preventing resin flow during cure, the separation of the chambers was made by edge breathing dams prepared by a sealant tape wrapped in carbon fibres. Both chambers were covered by a vacuum bag.

A wooden plate with a diameter of 140 mm was chosen as carrier for the whole set-up. As heating source a self-adhesive heating foil was placed between the glass tool and the wooden carrier. (Fig. 2). To monitor the temperature during the curing process, three thermocouples were attached on the bottom of the epoxy resin/ top of the glass tool (T1), at the top of the epoxy resin (T2) and at the barrier between the two chambers. The whole setup had to be able to perform a full 360° rotation, so all wires as well as the vacuum tube

were long enough to allow full rotation. To achieve the maximum resolution, the centre of rotation was exactly in the middle of the resin chamber. The whole setup is closed by polymer foam for temperature isolation to reach the necessary temperatures. Temperature control was performed manually using a variable power source to power the heating foil.

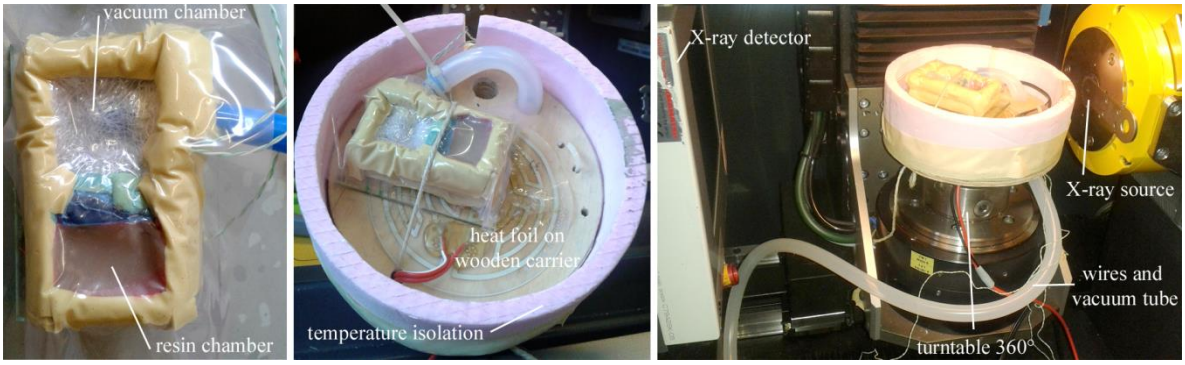

Fig. 2. Photograph's of the in-situ temperature-chamber within the Nanotom 180 NF XCT-device.

3. Results & Discussion

3.1 Preliminary Results

Before starting in-situ curing experiments in the XCT device, some preliminary investigations were performed. Using a syringe a water bubble was injected into an epoxy type 1 with a density of ~1.18 g/cm³. After water injection, this epoxy was fully cured in the laboratory. After curing, XCT scans were performed to detect this injected water bubble. After several attempts, no identification of the water within epoxy resin type 1 was possible. In a further step, the epoxy sample was put into a polypropylene (PP, density ~0.85 g/cm³) tube and filled with water. The results of these investigations are that the absorption contrast between epoxy type 1 and water is too low to clearly distinguish between these two phases. Further investigations with contrast medium to increase the absorption contrast of the injected water without influencing the properties of the water too much, were not successful. In a final step, epoxy type 2 (density of ~1.31 g/cm³) was chosen, which has a higher density than type 1. Fig. 3 clearly shows the differences in absorption contrast in frontal and axial XCT slices through epoxy type 1 and type 2, as well the corresponding unsigned 16 bit grey value histogram (right). For epoxy type 2 a clear separation between air, PP, water and epoxy was possible. In addition, in both epoxy types, air-voids are clearly observed.

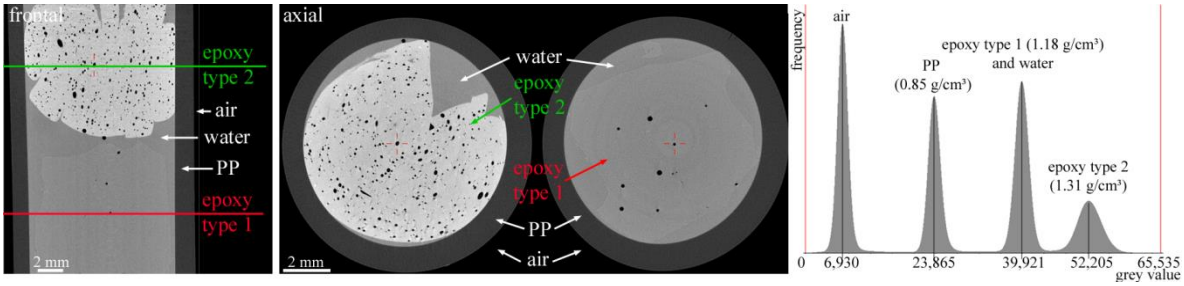

Fig. 3. Frontal (left picture) and axial (middle) XCT slices through epoxy type 1 and type 2 as well the corresponding grey value histogram (right) for air, polypropylene (PP), epoxy type 1, water and epoxy type 2. Voxel size: (8.1)³ µm.

3.2 In-Situ Investigations

Fig. 4 shows the temperature-time graphs for the first 160 minutes of our in-situ curing experiment. Temperature T1 indicates the temperature measured at the bottom of the resin (surface of the glass tool), and temperature T2 indicates the temperature at the top of the resin. Due to one-sided heating, a clear gradient with a maximum difference of approximately 45 °C between bottom and top of the resin is depicted. The red vertical lines indicate the individual time step, where the presented XCT images from Figs. 5-7 are located.

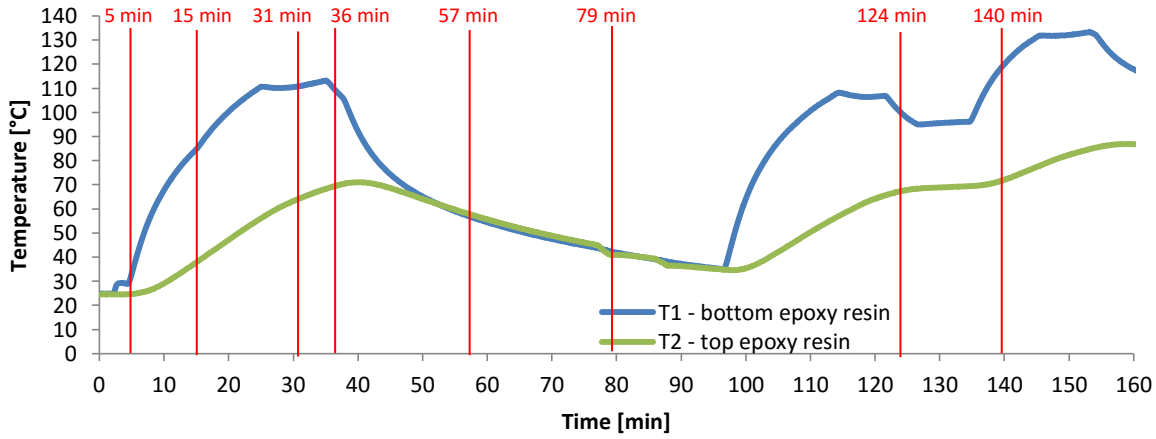

Fig. 4. Temperature-time graphs for the first 160 minutes of our in-situ curing experiments. The red vertical lines indicates the individual time step, were the presented XCT images from fig. 5-7 are located.

In Fig. 5 five reconstructed XCT slices of the first 57 minutes of in-situ curing are presented. Bright areas representing higher-absorbing sealant tape (#1) in front of the lower-absorbing wooden frame (#2). Due to the fact that for sample preparation the epoxy resin had to be pressed into our wooden frame, some initial air-pores (#3) are already present in the epoxy resin (#4) at the beginning of the curing process (t= 5 min). Due to pressing, the larger void has an elliptical shape. By increasing the temperature, the viscosity of the used epoxy resin decreases and this larger void starts to become spherical (t=15 min). The diameter of the larger air-bubble was approximately 1.7 mm. When the temperature of the epoxy resin increases further, the air-bubbles start moving upwards (t=31 & 36 min). Because of limited the measurement time of 5 minutes per scan, moving bubbles are blurred, compared to the static bubbles in the initial step. The air-bubbles moved upwards and were stopped at the surface of the epoxy resin by the covering vacuum bag. This first pre-heating phase of our in-situ investigations was necessary to reduce the amount of large voids in the middle of our sample for later water injection by a syringe.

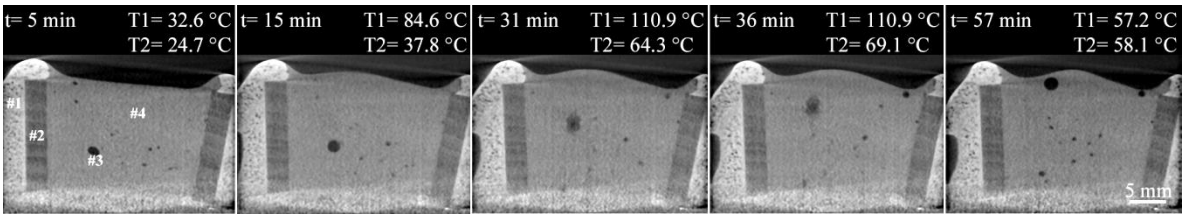

Fig. 5. XCT slices of epoxy resin (#4) with air-bubbles (#3) between a curing time of t= 5 min and t= 57 min. Bright areas representing higher absorbing sealant tape (#1) and the lower absorbing wooden frame (#2). Biggest void diameter ~1.7 mm, voxel size: $(58.7)^3$ µm.

Fig. 6 presents segmented air-bubbles in a frontal 3D-image within the whole volume of the investigated epoxy resin. At the beginning of the heating period, it is clearly

visible how the elliptical shape of the bubbles changes to a spherical shape. After that, the air-bubbles start moving upwards. In addition, some smaller voids start moving and join together with bigger ones.

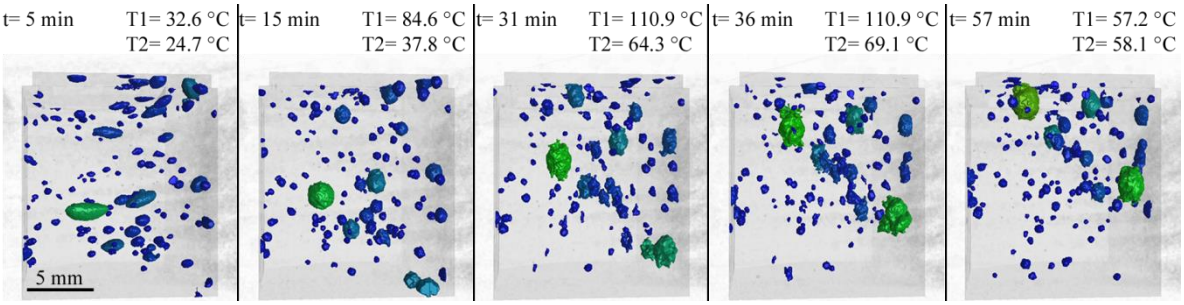

Fig. 6. Frontal 3D-view of segmented air-voids. The smaller pores are displayed in blue colour and the green ones have a diameter of ~1.7 mm as presented in Fig. 5. Voxel size: $(58.7)^3$ µm.

Fig. 7 depicts the first XCT scan after water injection by a syringe (t=79 min). Previous experiments have shown that for water injection the epoxy resin should have a temperature of approximately 40 °C. At this temperature the viscosity reaches a point where the injection of water is possible while keeping the movement of the water bubble within the resin low. The initial water-bubble is pear-shaped due to movement of the syringe upwards. As visible in the XCT scans, the contrast between water (#5) and epoxy resin (#4) is much lower compared to air-bubbles (#3). For better visualisation, the contrast of the images in the lower column was increased. Similar to the air-bubble, with increased epoxy temperature and reduced viscosity, the shape of the water-bubble changes to a sphere with a diameter of approximately 4.2 mm. Parallel to the change of shape, the water-bubble moves upwards until it is stopped by the vacuum bag.

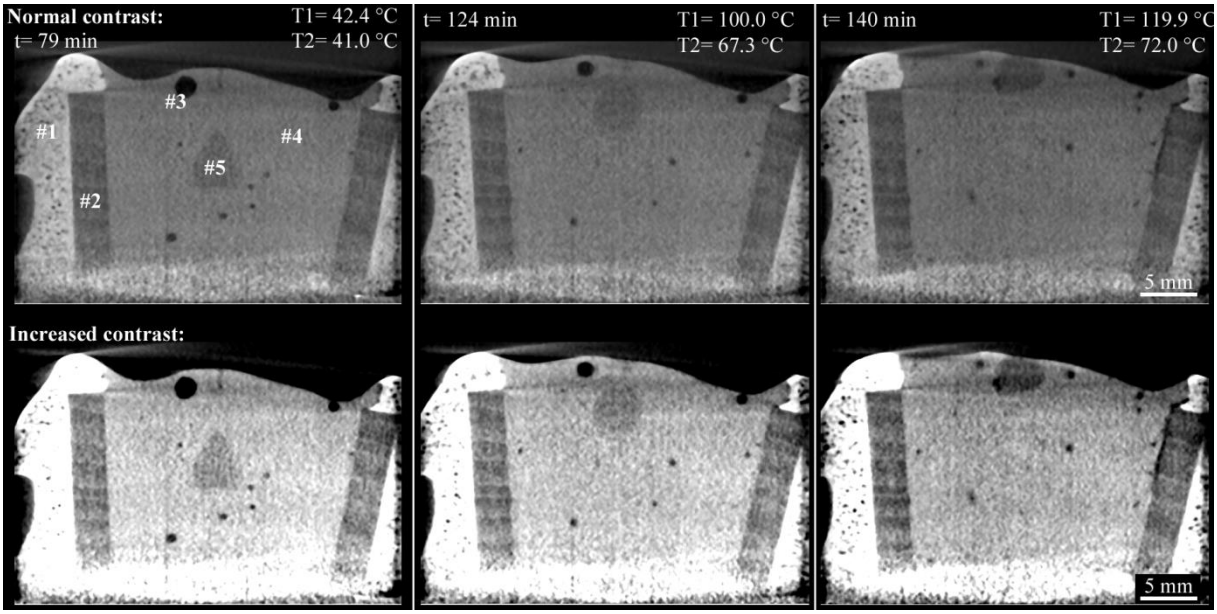

Fig. 7. XCT slices of epoxy resin (#4) after injection of a water-bubble (#5) between a curing time of t= 79 min and t= 140 min. Bright areas representing higher absorbing sealant tape (#1), the lower absorbing wooden frame (#2) and some remaining air-bubbles (#3). Water bubble diameter ~4.2 mm, voxel size: $(58.7)^3$ µm.

Due to limited contrast, reduced measurement quality, including artefacts from higher-absorbing materials close to the region of interest (e.g.: glass tool, sealing tape, thermo couples) and moving artefacts, segmentation and meaningful quantification of the water-bubble are a big challenge. Also, surrounding air-bubbles can lead to a miss

segmentation of the water-bubble. A semi-automatic segmentation of the water-bubble volume and calculation of the corresponding diameter between water injection (t= 79 min) and moving to the top surface of the sample (t ~140 min) has shown that the diameter increases from 3.8 mm to 4.3 mm [20].

In general the observed growth of the water-bubble over curing temperature conforms to theoretical studies from literature [5, 6, 14]. Main reasons for the growth are expansion according to the ideal gas law and not due to moisture absorbed in the resin. An initial drop in the water-bubble diameter at the beginning of the curing could not be observed. The compared mathematical models underestimated the growth rates which were observed with XCT [17]. For an exact comparison of the observed growth rate with mathematical models, a much more complex in-situ setup has to be built. Therefore, a more homogenous heating system, an exact measurement of the applied vacuum and pressure within the resin and the relative humidity level are necessary to be used as further input for mathematical models [17]. In addition, artefacts in XCT Data also lead to segmentation errors of the exact bubble volume and diameter. Investigations in this direction are planned for the future.

4. Conclusion and Outlook

In this work it was shown that commercially-available laboratory XCT systems are feasible for observation of air-bubbles in neat resin during curing process. If the density of the resin is in the range of ~1.3 g/cm³, the difference in absorption coefficients is high enough to detect water in resin. By injecting a water-bubble with a diameter of ~4.2 mm, the growth of the water-bubble over curing temperature could be observed. In general this effect is in conformity with theoretical studies from literature [5, 6, 14].

To reach the necessary scanning time of approximately 5 minutes per scan, compromises regarding XCT-resolution and image quality have to take into account compared to synchrotron sources. Avoiding higher absorbing components near the region of interest (e.g.: glass tool, sealing tape, thermo couples) can further reduce measurement artefacts.

Big advantage using a laboratory XCT system for in-situ experiments is the high availability and therefore the relative low costs to perform first feasibility studies of some special setups. Main limitations are the measurement times of approximately 5 minutes per scan. Therefore fast processes, as the movement of bubbles during curing can lead to motion blur. For a qualitative 3D evaluation, these artefacts can be ignored in a certain way. To obtain reliable quantitative values for the air- and water-bubbles, additional effort in data evaluation is necessary.

For future investigations a more practical in-situ set-up is planned including fibres within the resin or using prepreg material. For this set-up, it is assumed that the rise of the bubbles within a composite will be slowed down or even blocked by the fibre architecture. By applying recently developed software tools, individual features can be tracked. For example it can be easily distinguished between creation, continuation, split, merge and dissipation events [22]. Generated knowledge out of these investigations can lead to a better understanding of out-of-autoclave curing processes and can support the implementation of mathematical models in future software tools.

Acknowledgment

The work was financed by the K-Project ZPT+, supported by the COMET programme of FFG and by the federal government of Upper Austria and Styria. We would also like to thank Peter Orgill from University of Applied Sciences Upper Austria for proofreading.

References

[1] L. Farhang and G. Fernlund, “Void morphology, void evolution and gas transport in out-of-autoclave prepregs,” in Proceedings of the 26th Annual Technical Conference of the American Society for Composites, Montreal, QC, Canada, 26-28 September 2011.

[2] P. Olivier, J. Cottu, and B. Ferret, “Effects of cure cycle pressure and voids on some mechanical properties of carbon/epoxy laminates,” Composites, vol. 26, no. 7, pp. 509–515, 1995.

[3] E.A. Birt, R.A. Smith, A review of NDE methods for porosity measurement in fibre-reinforced polymer composites, Insight, 46 (11), pp. 681–686, 2004.

[4] A. Arafath and G. Fernlund, “Gas transport in prepregs: Model and permeability experiments,” in Proceedings of the 17th International Conference on Composite Materials, Edinburgh, UK, , pp. 1–10, 27-31 July 2009.

[5] Y. Ledru, G. Bernhart, R. Piquet, F. Schmidt, and L. Michel, “Coupled visco-mechanical and diffusion void growth modelling during composite curing,” Composites Science and Technology, vol. 70, no. 15, pp. 2139–2145, 2010.

[6] L.Grunenfelder and S.Nutt, “Void formation in composite prepregs–effect of dissolved moisture,” Composites Science and Technology, vol. 70, no. 16, pp. 2304–2309, 2010.

[7] T. Centea and P. Hubert, “The effect of material and process parameters on tow impregnation and micro-void formation in out-of-autoclave prepregs,” in Proceedings of the 26th ASC Conference, Montreal, QC, Canada, pp. 1279–1298, 26-28 September 2011.

[8] L. Farhang and G. Fernlund, “Void morphology, void evolution and gas transport in out-of-autoclave prepregs,” in Proceedings of the 26th Annual Technical Conference of the American Society for Composites, Montreal, QC, Canada, 26-28 September 2011.

[9] T. Centea, M. Preau, and P. Hubert, “Effect of layup and ply morphology on void formation in out-of-autoclave prepregs,” in Proceedigs of the 19th International Conference on Composite Materials, Montreal, QC, Canada, 28 July - 2 August 2013.

[10] L. Farhang and G. Fernlund, “Void evolution and gas transport during cure in out-of-autoclave prepreg laminates,” in Proceedings of the SAMPE Conference, Long Beach, CA, USA, pp. 1153: 1–12, 23-26 May 2011.

[11] H. Huang and R. Talreja, “Effects of void geometry on elastic properties of unidirectional fiber reinforced composites,” Composites Science and Technology, vol. 65, no. 13, pp. 1964–1981, 2005.

[12] B. Plank, G. Mayr, A. Reh, D. Kiefel, R. Stössel, J. Kastner - Evaluation and Visualisation of Shape Factors in Dependence of the Void Content within CFRP by Means of X-ray Computed Tomography - Proceedings of 11th European Conference on Non-Destructive Testing (ECNDT 2014), Prague, Czech Republic, pp. 9, 2014.

[13] B. Plank, G. Rao, J. Kastner - Evaluation of CFRP-Reference Samples for Porosity made by Drilling and Comparison with Industrial Porosity Samples by Means of Quantitative X-ray Computed Tomography - Proceedings 7th International Symposium for NDT in Aerospace, Bremen, Germany, pp. 10, 2015.

[14] J. Kardos, M. Dudukovi´c, and R. Dave, “Void growth and resin transport during processing of thermosetting - matrix composites,” in Epoxy resins and composites IV, Springer, pp. 101–123, 1986.

[15] J. R. Wood and M. G. Bader, “Void control for polymer-matrix composites (1): theoretical and experimentalmethods for determining the growth and collapse of gas bubbles,” Composites Manufacturing, vol. 5, no. 3, pp. 139– 147, 1994.

[16] R. Helmus, P. Hubert and R. Hinterhölzl ”Out-of-Autoclave Prepreg Consolidation – A Stochastic Approach to Model Void Formation”, in Proceedings of the 20th International Conference on Composite Materials, Copenhagen, Denmark, 2015.

[17] R. Helmus, Out-of-Autoclave Prepregs: Stochastic Modelling of Void Formation, Dissertation at Technical University of Munich, Institute for Carbon Composites, 2016.

[18] A. Taylor, B. Plank, G. Standfest, A. Petutschnigg - Beech wood shrinkage observed at the micro-scale by a time series of X-ray computed tomographs (µXCT) - HOLZFORSCHUNG, Vol. 67, No. 2, pp. 201-205, 2012.

[19] D. Salaberger, H. Scharleitner, J. Kastner - Analyse der Tinteausbreitung in Polymerschäumen mit Hilfe von Röntgen-Mikro Computertomografie - DACH ZfP Jahrestagung 2012, Graz, Österreich, 2012.

[20] M. Gschwandtner, Bubble Growth in Out-of-Autoclave (OoA) UD Prepreg During Processing, Bachelor's Thesis at Technical University of Munich, Institute for Carbon Composites, Nov. 2015.

[21] Cycom 5320-1 Epoxy Resin System - Technical Data Sheet (2012). URL: https://www.cytec.com/products/cycom-5320-1

[22] A. Reh, A. Amirkhanov, C. Heinzl, J. Kastner, E. Gröller - Fuzzy feature tracking: Visual analysis of industrial 4D-XCT data - COMPUTERS & GRAPHICS, Vol. 3, No. 1, pp. 177-184, 2015.